C. R. Mecanique 341 (2013) 462–468

Contents lists available at SciVerse ScienceDirect

Comptes Rendus Mecanique

www.sciencedirect.com

10th International Meeting on Thermodiffusion

Measurement of isothermal diffusion coefficients in ternary mixtures using counter flow diffusion cell

Aliaksandr Mialdun *, Viktar Yasnou, Valentina Shevtsova

Université libre de Bruxelles, Physical Chemistry Department, Microgravity Research Center, CP165/62, Av. Franklin-Delano-Roosevelt 50, B-1050 Brussels, Belgium

ARTICLE INFO

Article history:
Available online 22 February 2013

Keywords:
Diffusion
Ternary mixture
Injection
Mach–Zehnder interferometer
Common-path interferometer
Fitting

ABSTRACT

A new diffusion cell and an interferometer have been developed for determination of isothermal diffusion coefficients in ternary mixtures. Two interferometer schemes have been proposed and tested for the measurements. The classical Mach–Zehnder interferometer can be reconfigured into a common-path interferometer to resolve high gradients of the refractive index that are typical of diffusion experiments. Formulations, methodology and algorithms for data extraction are presented for the example of a ternary mixture with an equal mass fraction of all components (1:1:1) in the system of tetralin–isobutylbenzene–dodecane. The selection of the fitting procedure is very important for obtaining reliable results.

1. Introduction

The knowledge of mass transport (diffusion) coefficients is of great importance in many fields of science and technology. Our particular interest in measuring the isothermal diffusion originated from other studies of transport property of liquid mixtures, so-called thermal diffusion or Soret effect. The effect appears as a separation of mixture components in response to a thermal gradient. This effect is closely connected with diffusion, as both processes coexist; thermodiffusion tends to separate species, diffusion tends to homogenize them back and finally the system finds a steady state. Generally all coefficients characterizing both effects enter the mathematical model of the process simultaneously [1–3].

Only in a special type of experiments (like in a thermogravitational column), it is possible to determine directly the thermodiffusion coefficient from separation measurements at the steady state without knowledge of diffusion coefficients. But in most of the other cases one needs to consider both effects and to extract both types of coefficients at once. In binary mixtures, only two coefficients are sought and it does not pose any problem. The situation becomes worse in case of ternaries, as the system is controlled by two thermodiffusion coefficients and four Fickian diffusion coefficients [4,5]. Simultaneous fitting of a single experimental dataset with six parameters is practically hopeless. An approach developed to overcome the problem [6] consists in extracting additional information from the same experiment, for example, by applying a second probing wavelength [7]. This approach is under active development now and its reliability has to be thoroughly tested. For the above reason, an independent measurement of ternary diffusion coefficients as a supporting tool for extraction of correct thermodiffusion coefficients becomes extremely important.

The purpose of the present paper is to provide the development of a relatively simple, but flexible and accurate instrument for measuring isothermal diffusion coefficients by means of interferometry. The results of the test measurements are given for one ternary mixture in the system tetralin–isobutylbenzene–dodecane.

* Corresponding author.
E-mail addresses: amialdun@ulb.ac.be (A. Mialdun), vyasnou@ulb.ac.be (V. Yasnou), vshev@ulb.ac.be (V. Shevtsova).

1631-0721/$ – see front matter
http://dx.doi.org/10.1016/j.crme.2013.02.001

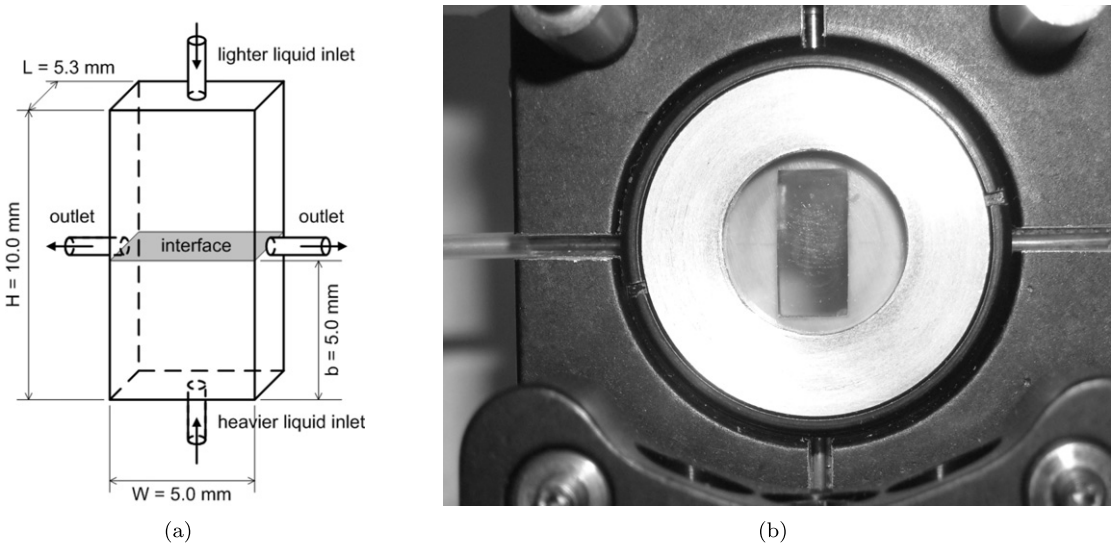

Fig. 1. The sketch of the cell (a) and the magnified photo of the cell (b).

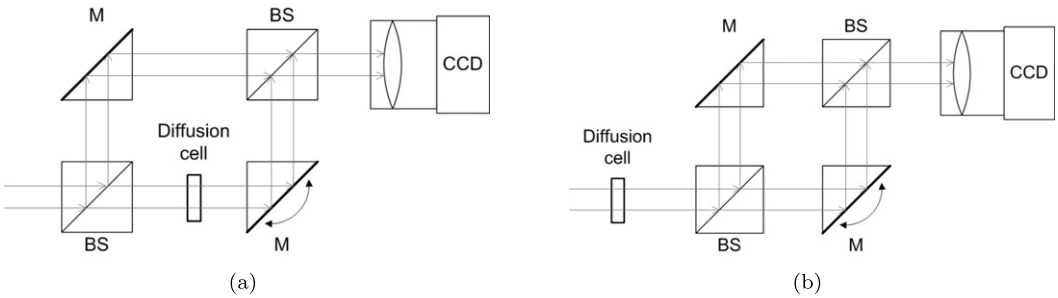

Fig. 2. Two different implementations of the interferometer. (a) Mach–Zehnder interferometer. (b) Common-path interferometer. (M – mirror, BS – beam splitter.)

2. Experimental section

2.1. Set-up

To measure diffusion by interferometric probing, we have developed a counterflow diffusion cell. The outer part of the cell is made of a brass disc of 25 mm diameter and 5 mm thick. A rectangular opening of 10 mm $\times$ 5 mm is cut in the disk, providing a volume to be filled with liquid. The disk is sandwiched between two glass windows 25.4 mm in diameter and 2 mm thick, with seals made of 0.15-mm-thick PTFE sheets between glass and brass. The whole assembly is mounted inside an optical holder for 1 inch lenses (black ring in Fig. 1(b)). Four channels aimed at injecting and removing the liquid from the cell are made of stainless steel capillaries 0.90 mm in outer diameter and 0.58 mm in inner diameter, and soldered into the brass disk. The inlet/outlet capillaries are equipped with valves to simplify injection and to block the liquid inside the cell before the experiment starts. Thus, the geometry of the cell is as follows (see Fig. 1(a)): the total diffusion path is $H = 10.0$ mm, the height of the interface is $b = 5.0$ mm and the length of the optical path in the liquid is $L = 5.30$ mm. A similar cell had been developed and successfully applied for accurate diffusion measurements in [8].

The cell and the interferometer were placed inside a box equipped with a system of active thermal control. The temperature inside the box was always kept at 298 K with residual fluctuations of ± 0.1 K (RMS value).

To observe the concentration variation inside liquid mixtures, different interferometric schemes are applicable; the most precise one is the phase-shifting technique (see, e.g., a good example of that in [9]). We have chosen and have tested two other types of interferometer schemes, which are: the classical Mach–Zehnder scheme and the common-path scheme (see Fig. 2). They are easy to implement and provide complete phase information from a single snapshot. Both are based on an identical set of components and differ only by the positioning of the cell with respect to the interferometer. In the Mach–Zehnder interferometer, the cell is located within an object arm inside the interferometer. In the common-path version, the cell is placed in front of the interferometer. The arms of the interferometer in this case are aligned in a special way, to create a small spatial vertical shift between both of them. The last scheme is particularly useful for diffusion experiments, as it allows resolution of steep refractivity gradients [10].

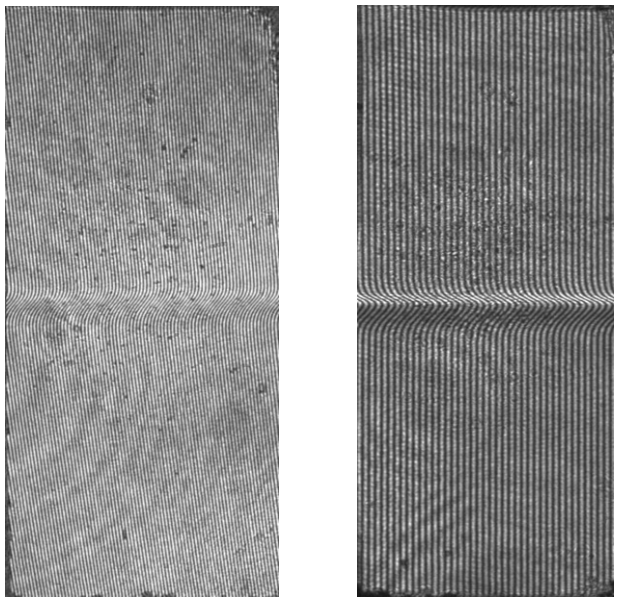

Fig. 3. Typical fringe patterns. (a) Mach–Zehnder interferometer. (b) Common-path interferometer.

The overall implementation of the interferometer is the same as that described in [11,12]. The light source is an expanded and collimated beam of a He–Ne laser with the wavelength $\lambda = 632.8$ nm. The resulting interferogram is recorded by a CCD camera with a sensor of 1280×1024 pixels size. The resolution of the imaging system is around 60 pixels/mm. The long-term phase stability is 0.1–0.2 rad.

2.2. Experimental procedure

The experimental procedure was as follows. The cell was filled through the bottom inlet, and then thermalization and stabilization of the interferometer and cell were continued for 8–10 hours. At the end of this phase, injection of another liquid was started through the top inlet. When the interface approached the outlets, injection from the bottom inlet was also activated. Both liquids flow for some time into the inlets and outlets to homogenize concentrations in the bulk of the two cell sections. Later in time, the injection speed was abruptly increased to make the interface sharp, then the injection was stopped, all the valves were closed and image recording was initiated. The image acquisition step was variable, often at the beginning of the experiment (each 10 s) and seldom by the end of the experiment (once per 300 s). Then the set of images was analysed to extract refractive index profiles. And finally, diffusion coefficients were evaluated by fitting an analytical solution to the obtained experimental data.

2.3. Image processing

In both interferometer implementations, image processing have been done by 2-D Fourier transform technique (see details, e.g., in [11]). For this reason, the interferometer was aligned to get a narrow fringe pattern. In both cases, the pictures of fringes are qualitatively different, as shown in Fig. 3. In all experiments fringe spacing has been adjusted to 4–6 pixels, although in the case of Fig. 3(b) it was made slightly higher for clarity of picture.

In spite of the basically same interferogram processing algorithm, the quantities extracted from the interference patterns for these interferometers are essentially different. In case of a classical Mach–Zehnder, the fringe pattern reflects an optical phase difference between reference and objective beams and can be expressed as:

$$\Delta\phi(x,z) = \phi(x,z) - \langle\phi(x,z)\rangle = \frac{2\pi L}{\lambda}\big[n(x,z) - n_0\big]$$

where $\langle\phi(x,z)\rangle$ is the phase value averaged over the full field of view and n_0 is the refractive index of a mixture with concentration averaged over the full cell volume. In this case, the phase difference extracted from the interferogram is straightforwardly transformed into the refractive index.

In a common-path interferometer, the fringe pattern is formed by the same object beam, but shifted with respect to itself for Δz step on the camera sensor; thus, in this case:

$$\Delta\phi(x,z) = \phi(x,z+\Delta z) - \phi(x,z) = \frac{2\pi L}{\lambda}\big[n(x,z+\Delta z) - n(x,z)\big] = \frac{2\pi L}{\lambda}\Delta z\frac{\partial n}{\partial z}$$

Taking images of the calibration target, produced by each individual beam, it is possible to accurately estimate Δz value. Afterwards, the gradient of the refractive index is calculated from the measured optical phase. In spite of certain advantages in measuring a refractive index gradient instead of plain refractivity, it requires either rewriting of an analytical solution describing the experiment, or integration of $\partial n/\partial z$ profile into $n(z)$.

In present experiments, the concentration differences between two solutions do not exceed 2 wt.% and the refractive index difference between the liquids is less than 2×10^{-3}. For this reason, the Mach–Zehnder interferometer has been chosen for the analysis of current diffusion measurement. Although we have not compared both schemes directly and did not use the common-path interferometer in the present study, we believe that mentioning this option is essential, as it allows easy adaptation of the set-up to steep concentration gradients that are untreatable by the classical Mach–Zehnder approach.

One of the important points in the interferometric measurements is the choice of a reference image. We have always chosen the last image of a series as a reference; concentration distribution over the cell is almost homogeneous at the end of diffusion relaxation, and even if some concentration difference is still present, it can be taken into account by a slight modification of the fitting formulations.

2.4. Data extraction

In a ternary mixture, two concentration variations contribute to the variation of the refractivity of fluid:

$$n(x,z) - n_0 = \left(\frac{\partial n}{\partial C_1}\right)_{C_2,T}\left[C_1(z,t) - C_1^0\right] + \left(\frac{\partial n}{\partial C_2}\right)_{C_1,T}\left[C_2(z,t) - C_2^0\right] \tag{1}$$

where $(\partial n/\partial C_i)$ are the so-called contrast factors, $C_i(z,t)$ is the spatial distribution of i-th component and C_i^0 is its mean value over the cell. Hereafter the following numbering of components is used: tetralin (THN) (1) – isobutylbenzene (IBB) (2) – dodecane (C12) (3). The values of the contrast factors needed to transform concentration distribution into refractive index were obtained by measuring the refractive index of a set of solutions around the concentration point of interest with an Abbe refractometer at 298 K and 670 nm wavelength (see [13] for details of the procedure). They are $(\partial n/\partial C_1) = 0.11709$ and $(\partial n/\partial C_2) = 0.07012$. Extrapolation of these values to the wavelength of interest gave a minor correction and therefore was not systematically applied.

One-wavelength diagnostics is applied to probe ternary mixture and it imposes additional problems. To fit the experimentally measured $n(z,t)$ profiles to Eq. (1), one needs an analytical solution for both concentrations. By use of the diffusion matrix diagonalization method [14] the solution derivation is rather straightforward:

$$\begin{pmatrix} C_1(z,t) - C_1^0 \\ C_2(z,t) - C_2^0 \end{pmatrix} = [P] \cdot \begin{bmatrix} f(z,t,\hat{D}_1) & 0 \\ 0 & f(z,t,\hat{D}_2) \end{bmatrix} \cdot [P]^{-1} \cdot \begin{pmatrix} C_1^{\mathrm{T}} - C_1^{\mathrm{B}} \\ C_2^{\mathrm{T}} - C_2^{\mathrm{B}} \end{pmatrix} \tag{2}$$

where $[P]$ is the modal matrix, whose elements are components of the eigenvectors of the diffusion matrix. One of the possible views of the modal matrix is, for example:

$$[P] = \begin{bmatrix} 1 & 1 \\ \frac{\hat{D}_1 - D_{11}}{D_{12}} & \frac{\hat{D}_2 - D_{11}}{D_{12}} \end{bmatrix} \tag{3}$$

Here D_{ij} are the components of diffusion matrix and $\hat{D}_i$ are the eigenvalues. C_i^{B} and C_i^{T} are the initial concentrations of i-th component in the bottom and top sections of the cell, respectively. Function $f(z,t,\hat{D}_i)$ is a solution of a binary diffusion problem with the same initial and boundary conditions and, in case of a diffusion cell, it can be written as:

$$f(z,t,D) = \frac{2}{\pi}\sum_{i=1}^{\infty}\frac{1}{n}\sin\left(\frac{n\pi b}{H}\right)\cos\left(\frac{n\pi z}{H}\right)\exp\left(-\frac{n^2\pi^2}{H^2}Dt\right) \tag{4}$$

Then, the solution for concentration profiles obtained by Eq. (2) with the help of Eqs. (3) and (4) are substituted into Eq. (1) and fitted to the experimental data.

In a real experiment, there are two issues that make experimental data deviating from a simple 1-D analytical solution. First, the initial distribution of the refractive index recorded in the experiment (and naturally assigned to the experiment time $t = 0$) does not have a perfect stepwise shape at liquids' interface as it is supposed to be according to the analytical solution. A reasonable approach to treat the problem is to introduce an initial time parameter t_0, which enters into the pool of fit parameters along with diffusion coefficients, since there is no way to estimate it *a priori*. In the presented experiments, this initial imperfection is well captured by $t_0 = 25$–50 s. Second, the reference image, although taken at the end of the experiment, may still keep trace of residual concentration. To eliminate the impact of the residual concentration, the very last calculated refractivity profile $\Delta n(z, t \to \infty)$ was either subtracted from all the calculated profiles with the following fit to pure experimental data, or, alternatively, was added to all experimental profiles with the following fit to pure calculated data. Application of these two corrections essentially improves the quality of the fit.

Table 1
Initial concentrations in two experiments measuring D_{ij} in the symmetric point (1:1:1).

Run No.	$C_1^{\mathrm{T}}/C_2^{\mathrm{T}}$	$C_1^{\mathrm{B}}/C_2^{\mathrm{B}}$	$\Delta C_1^{\mathrm{T-B}}$	$\Delta C_2^{\mathrm{T-B}}$	$\Delta n_{\mathrm{est}}/10^{-4}$	$\Delta n_{\mathrm{exp}}/10^{-4}$
1	0.31996/0.34001	0.33891/0.31991	−0.01895	0.02010	−8.06	−8.02
2	0.34006/0.31997	0.33994/0.34006	0.00012	−0.02009	−14.20	−14.17

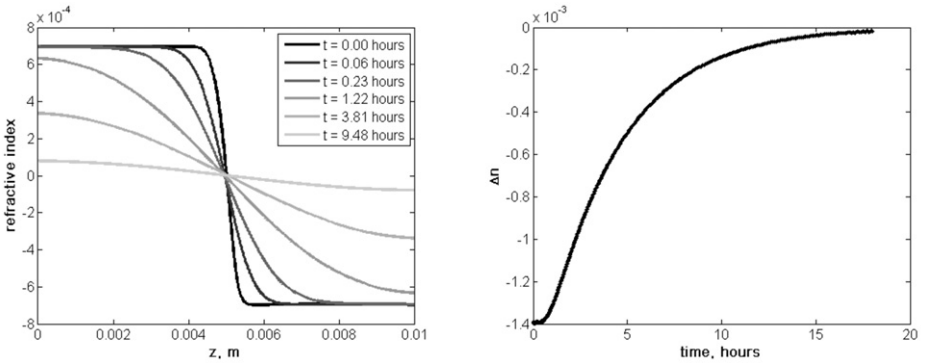

Fig. 4. Refractive index profiles measured in the experiment #2 (a); time evolution of the refractive index difference $\Delta n(t) = n_{z=H} - n_{z=0}$ in the same experiment (b).

3. Results and discussion

3.1. Experimental results

Two experiments were conducted to measure the diffusion coefficient in the mixture with equal mass fractions of components (1:1:1). The concentration of one of the three components was kept constant in each experiment. The concentrations of all mixtures in both experiments are listed in Table 1. In the first experiment, dodecane concentration was constant in both liquids; in the second experiment, tetralin concentration was kept constant. The evolution of refractive index profiles with time for the experiment #2 is shown in Fig. 4(a), while the time dependence of a total difference of the refractive indexes over the cell is shown in Fig. 4(b). Data consistency check is also provided in Table 1, where estimated refractive index differences calculated by known concentrations and contrast factors Δn_{est} have been compared with experimentally observed refractive index differences Δn_{exp}; both values coincide within less than 1%.

3.2. Diffusion coefficients

Fitting of single experiment (single run) generally does not provide reliable results, so we always fit the experimental data to the mathematical model for all available experiments simultaneously. In other words, all data obtained from all experimental runs have been fit to a single set of diffusion coefficients.

Two fitting procedures and their combination have been tested for the processing of the experimental data. The first is an unconstrained Nelder–Mead (simplex) method; the second is a trust region method. Both methods display some advantages and disadvantages, useful in one case and parasitic in another. The simplex method does not require information on an objective function shape or estimation of its gradients. It can explore larger regions in parametric space when looking for the minimum of the objective function. At the same time, it becomes less useful when the number of fit parameters is large. It can easily (repeatedly) converge toward a physically unreasonable result. The trust region method, on the contrary, estimates the shape of an objective function, approximating it by quadratic surface. This method usually needs a lesser number of iterations to converge, but it is true in case of a good initial guess. With a bad initial guess, it may not converge at all.

The searching process can be divided into a few steps, each one with its own objective and own best suited algorithm. The initial step can be aimed at searching for only diagonal elements of a diffusion matrix, assuming that cross-diagonal elements vanished. We have fixed D_{12} and D_{21} to 10^{-16} m^2/s and let only D_{11} and D_{22} vary. For this step, the optimization by the simplex method appeared as the fastest and most robust; it converged to the same values of diagonal elements independently of the initial guess. The obtained values are $D_{11} = 8.01 \times 10^{-10}$ m^2/s and $D_{22} = 7.25 \times 10^{-10}$ m^2/s. But, in the next step, when the above diagonal elements were provided as the initial guess for a 4-parameter fit, the simplex method often tended to converge to unreasonable values.

Table 2
Comparison of measured diffusion coefficients in the mixture THN–IBB–C12 with literature data.

Data source	Concentration, mass fraction	$D_{11}/10^{-10}$ m^2/s	$D_{12}/10^{-10}$ m^2/s	$D_{21}/10^{-10}$ m^2/s	$D_{22}/10^{-10}$ m^2/s	$\hat{D}_1/10^{-10}$ m^2/s	$\hat{D}_2/10^{-10}$ m^2/s
Galand et al. [15], run 1	0.46/0.24/0.30	11	9	11	58	60	9
Galand et al. [15], run 2	0.46/0.24/0.30	8.5	−13.1	−6.3	16.6	22.5	2.6
Königer et al. [7][a]	0.333/0.334/0.333	5.62	−5.91	1.08	12.18	10.99	6.81
Present study	0.333/0.333/0.334	6.92	1.06	−1.37	11.57	11.23	7.26

[a] Data have been transformed for the same order of the components.

The trust region method appears to be more robust in the case of a larger number of fit parameters and a better initial guess. The diffusion coefficients obtained by combination of the above methods somewhat differ from the initial guess and are listed in the last row of Table 2.

Diffusion coefficients for the same or close mixtures have been reported in literature recently [7,15]. In [7], diffusion coefficients are originally presented for another order of the components, namely for dodecane (1) – isobutylbenzene (2) – tetralin (3). After transformation of the diffusion matrix from C12–IBB–THN to THN–IBB–C12 order (transformation details have been provided in [7]), we got a set of data that are listed in the fourth row of Table 2. Paper [15] provides diffusion data for the same ternary system and, in spite of slightly different concentration, data from there were also taken for comparison. These data can be found in the second and third rows of the table. Results of [15] obtained by the open-ended capillary method demonstrate rather big scattering from run to run, too big values of some coefficients (see D_{22} for run 1), and very big both cross-diagonal coefficients, comparable to or even higher than diagonal ones. Such incoherence of the results in [15] can probably be explained by the fact that, in each case, all coefficients have been extracted from a single run (single diffusion couple), although it is worth to note that in one run (#2) of [15], values are close to realistic.

Results provided in [7] by two-wavelength probing of Soret separation are much closer to ours, although there are still some discrepancies. The worst thing is that misfit in diagonal D_{11} coefficient approaches 20%. Also cross-diagonal elements differ sometimes, not only in magnitude, but also in sign. But the good point is that eigenvalues in the present study and in [7] agree within 6%. For the moment, it is difficult to conclude about who's data are closer to the correct ones; the answer can come from either additional arbitration experiments or in-depth analysis of quality of diffusion experiments based on optical diagnostics, which can (and has to) be the subject of a separate study.

4. Conclusions

An instrument for the measurement of diffusion coefficients in ternary mixtures has been developed and tested in the system THN–IBB–C12 with equal mass fraction of components (1:1:1). The suggested interferometric scheme allows accurate measurement of the refractive index variation in the counterflow diffusion cell. The diffusion coefficients are determined by fitting the experimental results to an analytical solution. All experimental imperfections specific to the set-up can be treated by improvement of the experiment's model and corresponding modification of the fit procedure. Simultaneous fitting of few experimental runs with different diffusion couples allows more robust extraction of four diffusion coefficients.

Comparison of the results with the literature is quite confusing because of the different order of the components used in different papers. Researchers need to agree on the selection of the order of the components in the ternary mixtures.

In a recent paper [3], we suggested to choose a denser component as the first one, and then to reduce the density. The presented arguments look reasonable.

Acknowledgements

This work is supported by the PRODEX programme of the Belgian Federal Science Policy Office. The authors are thankful to Dr. V. Sechenyh and Prof. J.-C. Legros for the provided data on contrast factors; we are grateful to Prof. F. Dubois for valuable discussions.

References

[1] A. Mialdun, V. Shevtsova, Development of optical digital interferometry technique for measurement of thermodiffusion coefficients, Int. J. Heat Mass Tran. 51 (2008) 3164–3178.
[2] S. Wiegand, Thermal diffusion in liquid mixtures and polymer solutions, J. Phys.: Condens. Matter 16 (2004) 357–379.
[3] A. Mialdun, V. Yasnou, V. Shevtsova, A. Königer, W. Köhler, D. Alonso de Mezquia, M.M. Bou-Ali, A comprehensive study of diffusion, thermodiffusion, and Soret coefficients of water–isopropanol mixtures, J. Chem. Phys. 136 (2012) 244512.
[4] V. Shevtsova, V. Sechenyh, A. Nepomnyashchy, J.C. Legros, Analysis of the application of optical two-wavelength techniques to measurement of the Soret coefficients in ternary mixtures, Phil. Mag. 91 (2011) 3498–3518.
[5] P. Blanco, M.M. Bou-Ali, J.K. Platten, D.A. de Mezquia, J.A. Madariaga, C. Santamaria, Thermodiffusion coefficients of binary and ternary hydrocarbon mixtures, J. Chem. Phys. 132 (2010) 114506.
[6] K.B. Haugen, A. Firoozabadi, On measurement of molecular and thermal diffusion coefficients in multicomponent mixtures, J. Phys. Chem. B 110 (2006) 17678–17682.

[7] A. Königer, H. Wunderlich, W. Köhler, Measurement of diffusion and thermal diffusion in ternary fluid mixtures using a two-color optical beam deflection technique, J. Chem. Phys. 132 (2010) 174506.
[8] A. Komiya, S. Maruyama, Precise and short-time measurement method of mass diffusion coefficients, Exp. Therm. Fluid Sci. 30 (2006) 535–543.
[9] J. Torres, A. Komiya, E. Shoji, J. Okajima, S. Maruyama, Development of phase-shifting interferometry for measurement of isothermal diffusion coefficients in binary solutions, Opt. Lasers Eng. 50 (2012) 1287–1296.
[10] N. Rashidnia, R. Balasubramaniam, Measurement of the mass diffusivity of miscible liquids as a function of concentration using a common path shearing interferometer, Exp. Fluids 36 (2004) 619–626.
[11] A. Mialdun, V. Shevtsova, Measurement of the Soret and diffusion coefficients for benchmark binary mixtures by means of digital interferometry, J. Chem. Phys. 134 (2011) 044524.
[12] A. Mialdun, V. Shevtsova, Digital interferometry as a powerful tool to study the thermodiffusion effect, C. R. Mechanique 339 (2011) 362–368.
[13] V. Sechenyh, J.-C. Legros, V. Shevtsova, Experimental and predicted refractive index properties in ternary mixtures of associated liquids, J. Chem. Thermodyn. 43 (2011) 1700–1707.
[14] R. Taylor, R. Krishna, Multicomponent Mass Transfer, Wiley, New York, 1993.
[15] Q. Galand, S. Van Vaerenbergh, F. Montel, Measurement of diffusion coefficients in binary and ternary mixtures by the open ended capillary technique, Energ. Fuels 22 (2008) 770–774.